Revealing broad overlapping resonances by strong laser fields

Ilya Vorobeichik and Nimrod Moiseyev
Department of Chemistry and Minerva Center for Non Linear Physics, Technion, Israel Institute of Technology, Haifa 32000, Israel

(Received 24 July 1998)

The resonance states of a periodically driven barrier potential are investigated. We show that narrow shape-type resonances evolve from overlapping resonances of a static barrier as a result of an increase of the field amplitude. These shape-type resonances are associated with the field-induced barrier transparency phenomenon. It is suggested that cross-section experiments in strong laser fields may be used to uncover overlapping resonances. [S1050-2947(99)01902-2]

PACS number(s): 34.80.Qb, 73.40.Gk, 78.70.−g, 25.70.Ef

Tunneling through time periodically driven potential barriers has been intensively investigated in recent years, both theoretically and experimentally [1]. The dynamics of a driven system is governed by metastable states (resonances) that correspond to a temporary trapping of particles in the interaction region. Recently, it was demonstrated by Vorobeichik, Lefebvre, and Moiseyev that for a sufficiently strong field a single-barrier potential can become transparent for energies corresponding to the resonance states of an effective double barrier potential obtained upon one cycle averaging [2]. In the present work we investigate the resonances of a one-dimensional barrier potential driven by an external periodic force.

The Hamiltonian is given by

$$\hat{H}=\frac{p_x^2}{2m}+V(x)+\epsilon_0 x\sin(\omega t), \tag{1}$$

where

$$V(x)=V_0 e^{-ax^2}. \tag{2}$$

The potential for $V_0=0.0147$ a.u. (0.4 eV) and $a=5\times10^{-4}$ a.u.$^{-2}$ (1.787×10^{-3} Å^{-2}) is plotted in Fig. 1(a). These parameters are similar to ones used in Ref. [2], where the field-induced barrier transparency was demonstrated. They correspond to a semiconductor structure, such that the particle effective mass is $m=0.1$ a.u. (0.1 times the electron mass in vacuum) and $\hbar=1$. ϵ_0 and ω are the maximal field amplitude and the field frequency, respectively.

Let us first investigate the resonance states (which are associated with the poles of the scattering matrix) in the absence of the driving ($\epsilon_0=0$). In Fig. 1(a), the positions of the first three poles, $E_a-(i/2)\Gamma_a$, are shown by the horizontal dashed lines. The widths of these poles are very large, such that $\Gamma_a>|E_{a\pm1}-E_a|$. Such poles correspond to overlapping resonances. The resonance wave functions, obtained upon complex scaling [3], are shown in Fig. 1(b). They are localized inside the potential barrier and, therefore, in the classically forbidden region in phase space. These resonance states do not affect the scattering amplitude, and, therefore, have no physical meaning in one dimension. However, as recently demonstrated by Narevicius and Moiseyev [4], overlapping resonances of this kind become physical in two dimensions, and correspond to a temporary trapping of a light particle between two heavy particles.

The question we address here is what happens to these resonances when the periodic driving force is added. Since the Hamiltonian is time periodic [Eq. (1)], one can use the Floquet formalism. In this case, the solution of the time-dependent Schrödinger equation is given in terms of time-periodic Floquet states and quasienergies. The quasienergies $\mathcal{E}_n$ are the eigenvalues of the Floquet Hamiltonian

$$\left(-i\hbar\frac{\partial}{\partial t'}+H(x,t')\right)\Phi_n(x,t')=\mathcal{E}_n\Phi_n(x,t'), \tag{3}$$

where t' acts as an additional coordinate in the extended Hilbert space [5]. The resonance states of the driven system

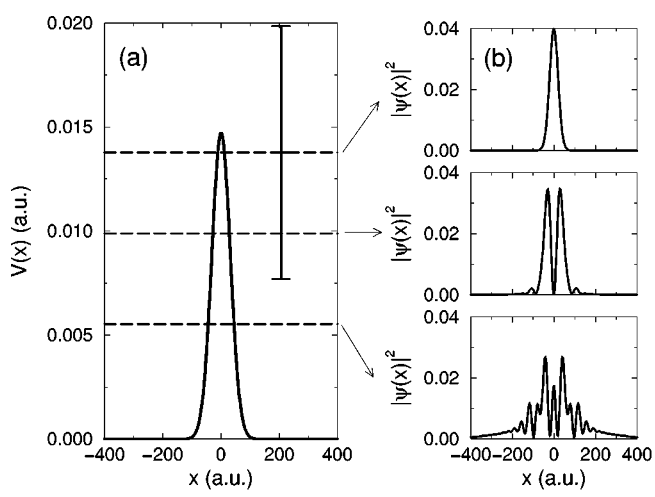

FIG. 1. (a) The potential barrier as defined in Eq. (2). Horizontal dashed lines stand for the positions of first three resonances with smallest width: $E_1=1.376\,839\times10^{-2}$ a.u., $E_2=9.883\,571\times10^{-3}$ a.u., and $E_3=5.533\,203\times10^{-3}$ a.u. The vertical line stands for the width of the first resonance, $\Gamma_1=1.214\,888\times10^{-2}$ a.u. The widths of the second and third resonances, $\Gamma_2=3.656\,166\times10^{-2}$ a.u. and $\Gamma_3=7.034\,301\times10^{-2}$ a.u., are not shown. The resonance states are obtained by analytical continuation of the coordinate to the complex plane ($x\to xe^{i\theta}$) [3], where $\theta=0.75$. (b) The wave functions of the three first resonance states obtained upon complex scaling for $\theta=0.75$ and grid spacing $\Delta x=2$ a.u.

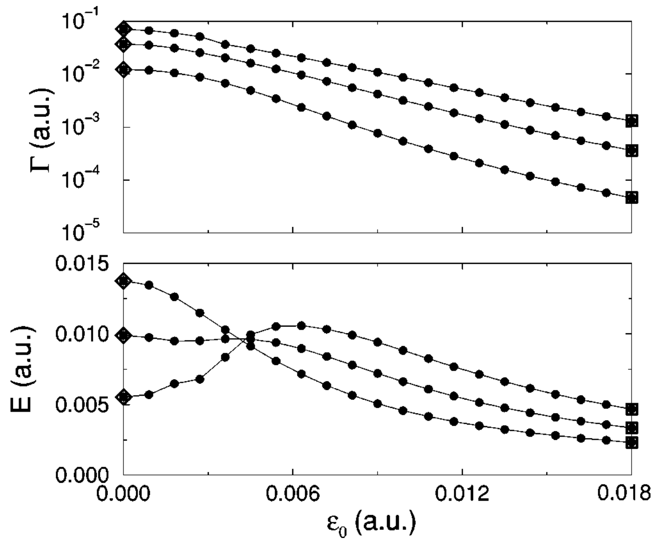

FIG. 2. The widths (Γ) and positions (E) of the first three resonances of a periodically driven barrier potential [Eq. (1)] as a function of the field amplitude ϵ_0 for $\omega = 0.03$ a.u. (filled circles). The solid lines that connect the resonances into trajectories were obtained by calculation of the maximal overlap of the resonance states at successive values of ϵ_0. The resonances were calculated by the complex scaled (t,t') method [6]. A one-period propagator matrix was constructed with 201 Fourier basis functions in the x coordinate $[\exp(in2\pi x/L), L = 2000$ a.u.$]$, five Fourier basis functions in the t' coordinate $[\exp(im\omega t')]$, and 250 time steps $[\tau = (2\pi/\omega)/250]$. The complex scaling parameter θ was changed linearly as a function of ϵ_0, such that $\theta(\epsilon_0 = 0) = 0.75$ and $\theta(\epsilon_0 = 0.018) = 0.36$. Rhombi (at $\epsilon_0 = 0$) stand for the widths and positions of the resonance states of a static barrier shown in Fig. 1. Squares (at $\epsilon_0 = 0.018$ a.u.) stand for the widths and positions of the resonance states of a one-period averaged effective potential shown in Fig. 3.

can be found by a complex scaling of the Floquet Hamiltonian. The complex scaling, combined with the (t,t') method [6] developed by Moiseyev and co-workers, can be used for effective calculation of the resonances, both for periodic and nonperiodic Hamiltonians.

In Fig. 2 the first three narrowest resonances of a driven Gaussian barrier are shown as a function of the field amplitude. The field frequency was held fixed at $\omega = 0.03$ a.u. Since the quasienergies are defined modulo $\hbar\omega$, they are mapped into the first Brillouin zone, i.e., $0 \leqslant \mathcal{E}_n \leqslant \hbar\omega$. As one can see from Fig. 2, as the field amplitude grows the resonance widths decrease dramatically. In addition, the resonance position is changed. In the absence of the driving $(\epsilon_0 = 0)$ the narrowest resonance has the highest position, but, for a sufficiently large field amplitude, the narrowest resonance has the lowest position. For sufficiently large ϵ_0 the resonances do not overlap, i.e., $\Gamma_a \ll |E_{a\pm1} - E_a|$. This interesting behavior can be explained using the oscillating frame representation of the Hamiltonian [7] in Eq. (1). In this representation (known as the Kramers-Henneberger representation) a pure time-dependent term, which physically is not important since it only yields an overall phase factor, is dropped. The Hamiltonian in this representation is given by

$$H(x,t) = \frac{p_x^2}{2m} + V[x + \alpha_0 \sin(\omega t)], \tag{4}$$

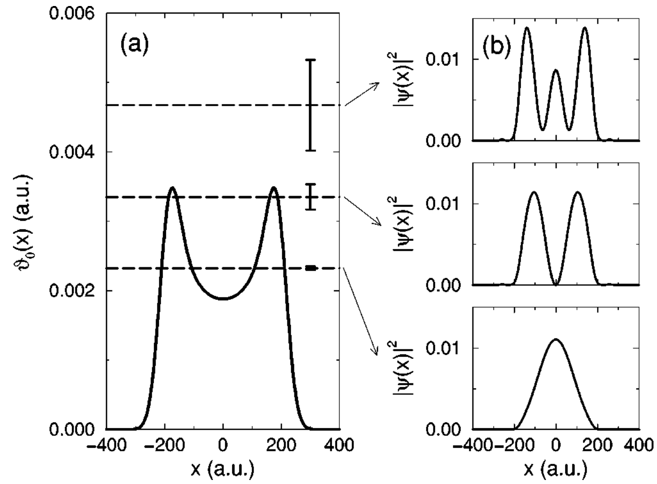

FIG. 3. (a) The one-period averaged effective potential as defined in Eq. (5) for $\alpha_0 = 200$ a.u. ($\epsilon_0 = 0.018$ a.u. and $\omega = 0.03$ a.u.). Horizontal dashed lines stand for the positions of the first three resonances with smallest widths, $E_1 = 2.324\,703 \times 10^{-3}$ a.u., $E_2 = 3.349\,674 \times 10^{-3}$ a.u., and $E_3 = 4.669\,356 \times 10^{-3}$ a.u. Vertical lines (''error bars'') stand for the widths of the resonances, $\Gamma_1 = 4.684\,349 \times 10^{-5}$ a.u., $\Gamma_2 = 3.641\,500 \times 10^{-4}$ a.u., and $\Gamma_3 = 1.309\,302 \times 10^{-3}$ a.u. (b) The wave functions of the three narrowest resonance states obtained upon complex scaling for $\theta = 0.36$ and a grid spacing of $\Delta x = 2$ a.u.

where $\alpha_0 = \epsilon_0 / m\omega^2$. The oscillating frame representation allows one to define an effective time-averaged potential

$$\mathcal{V}_0(x) = \frac{1}{T}\int_0^T V[x + \alpha_0 \sin(\omega t)]dt, \tag{5}$$

which, in the high-frequency limit, is a good approximation of a time-dependent system [8,2,9]. $\mathcal{V}_0(x)$ for $\epsilon_0 = 0.018$ a.u. is plotted in Fig. 3(a). As one can see, the effective potential is a double-well potential that supports typical shape-type resonances. The positions of the first three narrowest resonances in the effective potential are shown by horizontal dashed lines in Fig. 3(a), and the wave functions, obtained upon complex scaling, are shown in Fig. 3(b). The resonances are nonoverlapping, and the corresponding wave functions are localized in the classically allowed region of phase space. These resonance states have a large effect on the scattering amplitude. In the case of narrow resonances, if the energy of the incoming particles coincides with the resonance position, then a total transition through the barrier is obtained. Moreover, as shown recently [2], a single-barrier potential can also become transparent when the field frequency ω is larger than the frequency of a particle motion in the one-period averaged effective potential, Ω. In this case, the resonance states of a driven system are very similar to the resonances states of the effective potential. Therefore, by analyzing the shape of the effective potential as a function of ϵ_0, one can explain the source of the resonances shown in Fig. 2. As one increases the field amplitude, the effective potential changes. For a sufficiently large value of ϵ_0 it becomes a double-well potential. Therefore, by changing the field amplitude adiabatically one can reveal the broad overlapping resonances of the static potential (shown by rhombi in Fig. 2) that evolve into narrow resonances which are as-

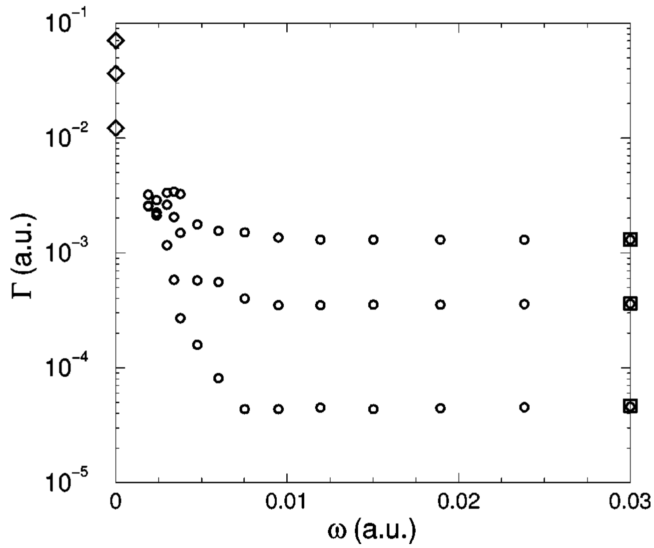

FIG. 4. The widths of the first three resonances of a periodically driven barrier potential [Eq. (1)] as a function of the field frequency ω for $\alpha_0=200$ a.u. For each field frequency the complex scaling parameter was optimized such that $\partial[E_a-(i/2)\Gamma_a]/\partial\theta$ was minimal. Rhombi (at $\omega=0$) stand for the widths of the resonance states of a static barrier shown in Fig. 1. Squares (at $\omega=0.03$ a.u.) stand for the widths of the resonance states of a one-period averaged effective potential shown in Fig. 3.

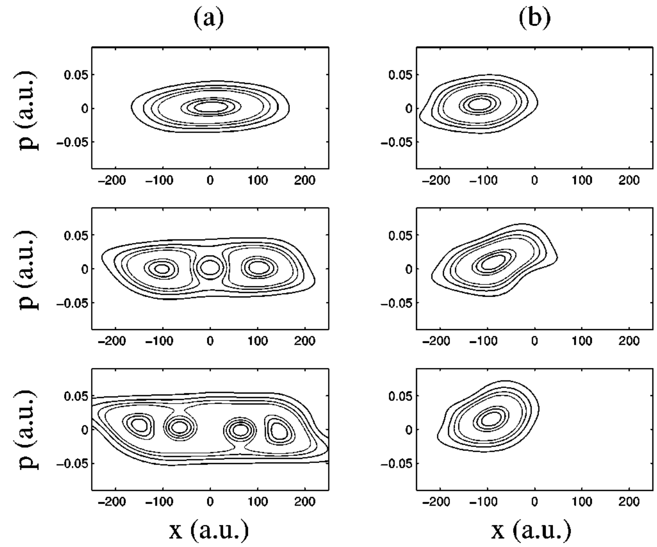

FIG. 5. The Husimi distribution [Eq. (6)] of the resonance wave functions in the driven barrier potential defined in Eq. (1) for $\alpha_0=200$ a.u. and $\sigma=5\times10^{-4}$ (a) for driving frequency $\omega=0.03$ a.u. and (b) for driving frequency $\omega=0.0019$ a.u. (the smallest laser frequency in Fig. 4).

sociated with the effective double-well potential (shown by squares in Fig. 2). Since the positions of the resonances in the two limits are exchanged as ϵ_0 is varied, they should cross for a certain value of the field amplitude. This happens when the effective potential is nearly harmonic for the relevant range of energies. The resonance states of a harmonic barrier can be calculated analytically. They all have the same position $[E=V(x=0)]$, and their widths differ by the oscillator frequency. For larger field amplitudes, the effective potential is not harmonic and the double-barrier structure appears. As one can see, *high-frequency lasers can be used to reveal the unphysical resonances of a static barrier that become physically accessible as one increases the field amplitude*. Narrow resonances are obtained when $\alpha_0=\epsilon_0/m\omega^2$ is sufficiently larger than the barrier width. Therefore, the limitation of large α_0 and high frequency may result in very large field amplitudes for which a physical realization of the phenomenon will become impossible. Therefore, it is important to investigate how the resonance states of a driving barrier depend on the field frequency. Since the effective potential is only α_0 dependent, we calculate the resonance states by varying ϵ_0 and ω such that $\alpha_0=\epsilon_0/m\omega^2$ is held fixed.

In Fig. 4 the widths of the first three resonances of the driven barrier as a function of the laser frequency for $\alpha_0=200$ a.u. are shown. The resonance states of the effective potential are the same as in Fig. 3, and their widths are shown by squares at $\omega=0.03$ a.u. As one can see, in the range 0.01 a.u.$<\omega<$0.03 a.u., the resonances of the effective potential are very similar to the resonances of the driven barrier. These laser frequencies are much larger than the frequency of the particle trapped in the one-period averaged effective potential ($\Omega\simeq0.001$ a.u. for $\alpha_0=200$ a.u., in our studied case). Therefore, in this range of frequencies, a field-induced barrier transparency will be obtained. However, for smaller laser frequencies, the resonances widths change and they overlap. Eventually, at $\omega\simeq0.025$ a.u., the resonances have about the same width. This happens since, in the small-field frequency case, the coupling between different Floquet channels is very large and the resonance states are strongly coupled one to another. To illustrate this, in Fig. 5 we compare the Husimi distribution of the resonance states of the driven barrier for $\omega=0.03$ a.u. [Fig. 5(a)] and for $\omega=0.0019$ a.u. [Fig. 5(b)]. (We were unable to calculate the resonances for smaller laser frequencies, due to numerical difficulties.) The Husimi distribution is defined as [10]

$$G(x_0,p_0)=\left|\left(\frac{\sigma}{\pi\hbar}\right)^{1/4}\int_{-\infty}^{\infty}e^{-[\sigma(x-x_0)^2/2\hbar]+i(p_0/\hbar)x}\Psi(x)dx\right|^2. \tag{6}$$

In our case, $\Psi(x)$ is the resonance complex scaled Floquet wave function at $t=n2\pi/\omega$ $(n=0,1,2,\dots)$ obtained by a diagonalization of a one-period propagator. For the complex-scaled functions, the x coordinate in Eq. (6) is replaced by a complex one, $xe^{i\theta}$.

In Fig. 5, the Husimi distributions of the Floquet resonance states are shown. They are not symmetric for $x\to-x$ and $p\to-p$, since this symmetry is of the field-free Hamiltonian and not of the time-dependent Hamiltonian given in Eq. (1). As one can see in Fig. 5(a), Husimi distributions of the three resonances of a driven barrier for $\omega=0.03$ a.u. are different from one another. However, for $\omega=0.0019$ a.u. [Fig. 5(b)], Husimi distributions of all three resonances are very similar, and they only differ by phases. This might be a result of a strong coupling between different resonance states. Such states have previously been found to be associated with the classical chaotic dynamics of similar systems, and can be referred to as "chaotic quasienergy states" [11]. Indeed, by analyzing the classical phase space of the driven barrier for the parameters of Fig. 4, one obtains that for frequencies smaller than 0.01 a.u. a mixed regular-chaotic dynamics is obtained. For very small driving frequencies ($\omega < 0.003$ a.u.), one cannot use the classical phase-space plots, since the classical particle escapes from the interaction region during a time that is smaller than one period of the driving force.

In conclusion, we have shown that the resonance states of a driven barrier are very different in high- and low-frequency limits. The resonance structure in the high-frequency limit can be understood by using an oscillating frame representation of the Hamiltonian. For sufficiently high frequency and a large-amplitude field, narrow resonances states are obtained, leading to a pronounced structure in the scattering cross section. In the low-frequency limit, the resonance states overlap, and are strongly coupled to one another. In such a case, a field-induced barrier transparency is not obtained. In this limit, however, the behavior of the resonance states is intriguing and worth further investigation. In previously studied cases [12] it was shown that it is very difficult (if at all possible) to trace the overlapping resonances experimentally. We suggest a way to uncover the overlapping resonances. We have shown in this Brief Report that such resonances states can be revealed by carrying out cross-section scattering experiments in strong laser fields.

This work was supported by the Israel-U.S.A. Binational Science Foundation, and by the fund for the promotion of research at the Technion.

[1] R. Ferreira and G. Bastard, Rep. Prog. Phys. **60**, 345 (1997), and references therein; A. K. Kazanskii, V. N. Ostrovskii, and E. A. Solov'ev, Zh. Éksp. Teor. Fiz. **70**, 493 (1976) [Sov. Phys. JETP **43**, 254 (1976)]; M. Holthaus and D. Hone, Phys. Rev. B **47**, 6499 (1993); M. Wagner, Phys. Status Solidi B **204**, 382 (1997); M. Ya. Azbel' and V. M. Tsukernik, Europhys. Lett. **41**, 7 (1998).

[2] I. Vorobeichik, R. Lefebvre, and N. Moiseyev, Europhys. Lett. **41**, 111 (1998).

[3] N. Moiseyev, Phys. Rep. **302**, 211 (1998), and references therein; W. P. Reinhardt, Annu. Rev. Phys. Chem. **33**, 223 (1982).

[4] E. Narevicius and N. Moiseyev, Mol. Phys. **94**, 897 (1998).

[5] H. Sambe, Phys. Rev. A **7**, 2203 (1973); J. S. Howland, J. Math. Phys. **24**, 1240 (1983).

[6] U. Peskin and N. Moiseyev, J. Chem. Phys. **99**, 4590 (1993); N. Moiseyev, Int. J. Quantum Chem. **63**, 279 (1997).

[7] H. A. Kramers, *Quantum Mechanics* (North-Holland, Amsterdam, 1956); W. C. Henneberger, Phys. Rev. Lett. **21**, 838 (1968).

[8] *Atoms in Intense Laser Fields*, edited by M. Gavrila (Academic, New York, 1992).

[9] V. Averbukh and N. Moiseyev, Phys. Rev. A **57**, 1345 (1998); I. Vorobeichik and N. Moiseyev, Phys. Rev. A (to be published).

[10] K. Husimi, Proc. Phys. Math. Soc. Jpn. **22**, 264 (1940).

[11] N. Ben-Tal, N. Moiseyev, and H. J. Korsch, Phys. Rev. A **46**, 1669 (1992).

[12] E. Narevicius and N. Moiseyev, Chem. Phys. Lett. **287**, 250 (1998); A. Garcia-Vela, R. B. Gerber, D. G. Imre, and J. J. Valentini, Phys. Rev. Lett. **71**, 931 (1993); A. Garcia-Vela, R. B. Gerber, D. G. Imre, and J. J. Valentini, Chem. Phys. Lett. **202**, 473 (1993); T. Schröder, R. Schinke, M. Mandziuk, and Z. Bačić, J. Chem. Phys. **100**, 7239 (1994); T. Schröder, R. Schinke, and Z. Bačić, Chem. Phys. Lett. **235**, 316 (1995).